13th World Conference on Earthquake Engineering
Vancouver, B.C., Canada
August 1-6, 2004
Paper No. 545

APPLICATION OF THE MODAL PUSHOVER PROCEDURE TO ESTIMATE NONLINEAR RESPONSE ENVELOPES

K. TOKORO[1], C. MENUN[2]

SUMMARY

Traditional nonlinear static pushover analyses cannot fully address the multi-mode effects and response interaction that occur in a seismically excited structure. The recently developed modal pushover analysis (MPA) procedure improves on traditional pushover analyses by including multi-modal effects; however, its application is currently restricted to predicting the peak values of scalar response quantities. The peak responses computed using the MPA procedure could be used to form a rectangular demand envelope for any two specified response quantities. However, this rectangular envelope may be overly conservative as compared to the corresponding values computed by nonlinear time-history analyses. This paper describes a procedure, which uses the results of MPA analyses, to predict the envelope that bounds a vector of responses in a nonlinear structure. The accuracy of the proposed procedure is examined for selected pairs of responses by comparing the predicted envelope to the mean simulated response envelope obtained from an ensemble of nonlinear dynamic analyses. The response pairs considered include bi-directional inter-story drifts and bending-moment-axial-load interaction in columns within a three-dimensional model of a three-story steel-moment-resisting-frame building. It is shown that the procedure has a level of accuracy that is appropriate for estimating the impact of seismic response interaction on the performance of a structure loaded into its nonlinear range.

INTRODUCTION

The necessary size and strength of a seismically-loaded structural component is often controlled by the simultaneous action of two or more loads and/or deformation demands (collectively called response quantities in this paper). For example, a column in a moment frame must be proportioned to resist an axial force and bending moment that act concurrently and vary in time. For any specified combination of responses, the adequacy of the element to resist those responses is usually ascertained using an interaction diagram, which defines the boundary between the safe and unsafe response combinations. Most of the commonly used interaction diagrams, such as those associated with moment-axial interaction in steel or reinforced concrete columns, have remained relatively unchanged for many years, suggesting that the capacity of structural elements subjected to interacting responses is well understood. However, to use

[1] Graduate Student, Stanford University, Stanford, USA. Email: tokoro@stanford.edu
[2] Assistant Professor, Stanford University, Stanford, USA. Email: menun@stanford.edu

these interaction diagrams effectively with seismically-loaded elements, the engineer must also have reliable estimates of the peak values of the responses and a model for the correlation that exists between them, since it is often observed that the critical response combination that occurs in an element during an earthquake does not include the peak value of any of the responses.

It is common in the current practice to estimate the peak values of seismic response quantities using the nonlinear static procedure (NSP) prescribed by FEMA 273 [1]; however, it is well known that this procedure is not well suited to responses that receive significant contributions from more than one mode of vibration. To address this problem with the conventional NSP, Chopra [2] proposed the modal pushover analysis (MPA) procedure, which combines the contributions from multiple modes of vibration to the peak value of a response quantity by a square-root-sum-of-squares (SRSS) rule similar to that used in conventional response spectrum analyses. Chopra [2] has demonstrated that, for several response quantities commonly used to assess the seismic performance of a structure, the MPA procedure has a level of accuracy that is comparable to that of response-spectrum-based analyses performed on linear structures.

Unfortunately, neither the NSP nor the MPA procedure provides any indication of the correlation between two response quantities in time. Consequently, for elements controlled by response interaction, it is common in the current practice to use the estimates of the individual response maxima provided by the NSP or MPA procedures to construct a rectangular envelope, which is compared to the interaction diagram of the element. However, this practice, which implicitly assumes that the responses are perfectly correlated, can be overly conservative, as illustrated by Menun [3] for structures responding in their linear-elastic range. To address this problem in linear structures, Menun [4] developed a response-spectrum-based procedure for predicting the envelope that bounds two or more seismic responses as they evolve in time. In this paper, we modify this linear response-spectrum-based envelope for use with structural systems possessing material nonlinearities by incorporating the results provided by MPA analyses.

In addition to moment-axial interaction in columns cited above, the simultaneous action of two or more seismic responses must also be considered when, e.g., (1) sizing anchor bolts for combined shear and tensile forces, (2) proportioning coupled shear walls in elevator cores for axial load and overturning moments, or (3) estimating the maximum bi-directional inter-story drifts in any direction in torsionally-excited buildings. In this paper, we focus our attention on the envelopes that bound (1) the bi-directional inter-story drifts and (2) the axial forces and bending moments in selected columns of a three-story steel-moment-resisting-frame building to demonstrate the accuracy of the proposed procedure, which is quantified by comparing the predicted envelope to the mean simulated response envelope obtained from an ensemble of nonlinear dynamic analyses. These comparisons serve to demonstrate that the proposed procedure, while not as accurate as the existing response-spectrum-based procedure available for linear structures, does provide a reasonable estimate for the envelope that bounds a pair of seismic responses in a nonlinear structure that is appropriate for structural design and analysis.

PROPOSED ENVELOPE

Central to the development of the proposed envelope is the response-spectrum-based envelope derived by Menun [4] for linear structures. This linear envelope is modified for use with nonlinear structures by replacing the conventional response-spectrum-based estimates for the peak modal earthquake-induced responses assumed in its formulation with the peak modal responses predicted by the MPA procedure developed by Chopra [2]. In this section, we summarize the details of linear response-spectrum-based envelope and the necessary modifications to incorporate nonlinear response.

Response-spectrum-based envelope for linear structures

The response spectrum method is commonly used to predict the peak values of seismic response quantities in linear structures. To employ this method, an eigenvalue analysis of the structure model is first performed to identify its natural modes of vibration. For each significant mode, the peak value of a response quantity of interest is computed using a prescribed set of design response spectra. The modal maxima are then combined using a suitable modal combination rule to estimate the maximum value of the response. Menun [4] extended the conventional response spectrum method for use in predicting the envelope that bounds a vector response process as it evolves in time. A summary of the derivation of this linear envelope necessary for the subsequent development of an envelope suitable for bounding responses in nonlinear structures is presented in this section. For brevity, we restrict the following derivation to the case of two response quantities; however, we remark that the procedure can be easily extended to any number of responses if desired. The interested reader is referred to reference [4] for additional details.

Consider an N-degree-of-freedom linear and classically damped structure with $n \leq N$ significant modes of vibration and let $\mathbf{x}(t) = [x_1(\mathrm{t}), x_2(t)]^T$ denote a vector of time-varying responses. In general, $\mathbf{x}(t) = \mathbf{x}_O + \mathbf{x}_Q(t)$, where $\mathbf{x}_O$ is the 2×1 vector of responses caused by static loads acting on the structure and $\mathbf{x}_Q(t)$ is the 2×1 vector of seismic responses. Each element of $\mathbf{x}(t)$ can be expressed as a linear function of the nodal displacements of the structure, $\mathbf{u}(t) = [u_1(t), u_2(t),\ldots,u_N(t)]^T$; i.e., $x_r(t) = \mathbf{q}_r^T\mathbf{u}(t)$, where the elements of the N-vectors $\mathbf{q}_r^T$, r = 1,2 are functions of the stiffness and undeformed geometry of the structure. When static and seismic loads act concurrently on the structure, $\mathbf{u}(t) = \mathbf{u}_O + \mathbf{u}_Q(t)$, where $\mathbf{u}_O$ and $\mathbf{u}_Q(t)$ are the N-vectors of nodal displacements caused by the static and seismic loads, respectively. Thus, $x_r(t) = \mathbf{q}_r^T[\mathbf{u}_O + \mathbf{u}_Q(t)] = x_{Or} + x_{Qr}(t)$, where

$$x_{Or} = \mathbf{q}_r^T \mathbf{u}_O \tag{1}$$

and

$$x_{Qr}(t) = \mathbf{q}_r^T \mathbf{u}_Q(t) \tag{2}$$

are the rth elements of $\mathbf{x}_O$ and $\mathbf{x}_Q(t)$, respectively.

When the structure is subjected to three translational components of ground motion, $\mathbf{u}_Q(t)$ can be expressed in a modal superposition form

$$\mathbf{u}_Q(t) = \sum_{k=1}^{3}\sum_{i=1}^{n} \boldsymbol{\varphi}_i \gamma_{ki} d_{ki}(t) \tag{3}$$

where $\boldsymbol{\varphi}_i$ is the ith mode shape, $d_{ki}(t)$ is the relative displacement response of an oscillator that has frequency, ω_i, and damping ratio, ζ_i, of mode i when it is subjected to the kth component of ground motion and

$$\gamma_{ki} = \frac{\boldsymbol{\varphi}_i^T \mathbf{M} \boldsymbol{\iota}_k}{\boldsymbol{\varphi}_i^T \mathbf{M} \boldsymbol{\varphi}_i} \tag{4}$$

is the participation factor associated with the ith mode and kth component of ground motion. In (4), $\mathbf{M}$ is the mass matrix and $\boldsymbol{\iota}_k$ is the influence vector that represents the displacement of the nodal masses resulting from the static application of a unit ground displacement in the kth direction. Substituting (3) into (2) yields the modal decomposition

$$x_{Qr}(t) = \mathbf{q}_r^T \sum_{k=1}^{3}\sum_{i=1}^{n} \boldsymbol{\varphi}_i \gamma_{ki} d_{ki}(t), \qquad r = 1,2. \tag{5}$$

Using (5) as a basis, the peak value $X_r = \max |x_{Qr}(t)|$ is estimated by the response spectrum method as

$$X_r^2 = \sum_{k=1}^{3}\sum_{i=1}^{n}\sum_{j=1}^{n} (\mathbf{q}_r^T \boldsymbol{\varphi}_i \gamma_{ki})(\mathbf{q}_r^T \boldsymbol{\varphi}_j \gamma_{kj}) \rho_{ij} D_{ki} D_{kj}, \qquad r = 1,2 \tag{6}$$

in which $D_{ki} = \max| d_{ki}(t) |$ is the displacement response spectrum ordinate corresponding to mode i and ρ_{ij} denotes the correlation coefficient between responses in modes i and j. In deriving (6), it is assumed that the components of ground motion are uncorrelated in the directions that they are applied to the structure. The necessary modifications to (6) for the case when the components of ground motion are correlated are described in reference [4]. As indicated in reference [4], to formulate the response-spectrum-based envelope bounding $x_{Qr}(t)$ and $x_{Qs}(t)$, we must also evaluate the cross term

$$X_{rs} = \sum_{k=1}^{3}\sum_{i=1}^{n}\sum_{j=1}^{n}(\mathbf{q}_r^T\boldsymbol{\varphi}_i\gamma_{ki})(\mathbf{q}_s^T\boldsymbol{\varphi}_j\gamma_{kj})\rho_{ij}D_{ki}D_{kj}\ , \tag{7}$$

which is related to the covariance between $x_{Qr}(t)$ and $x_{Qs}(t)$ and carries the information needed to quantify the correlation between these responses. Note that (6) is a special case of (7) with $r = s$, i.e., $X_{rr} = X_r^2$ is the square of the response spectrum method estimate of the maximum value of $x_{Qr}(t)$. Furthermore, it is apparent from (7) that $X_{rs} = X_{sr}$.

For the subsequent derivations, it is convenient to define

$$X_{rki} = \mathbf{q}_r^T\boldsymbol{\varphi}_i\gamma_{ki}D_{ki}\ , \qquad r = 1,2 \tag{8}$$

which represents the response-spectrum-based estimate of the peak ith mode response of $x_{Qr}(t)$ when the structure is subjected to the kth component of ground motion. Chopra [5, pp 516-559] shows that X_{rki} is in fact the value of response x_r when the structure is statically loaded with the force vector $\mathbf{s}_{ki}A_{ki}$, where $\mathbf{s}_{ki} = \gamma_{ki}\mathbf{M}\boldsymbol{\varphi}_i$ and $A_{ki} = \omega_i^2 D_{ki}$ are the inertial force distribution vector and pseudo-acceleration response spectrum ordinate associated with the ith mode of vibration and kth component of ground motion, respectively. Substituting (8) into (7) yields

$$X_{rs} = \sum_{k=1}^{3}\sum_{i=1}^{n}\sum_{j=1}^{n} X_{rki}X_{skj}\rho_{ij}\ . \tag{9}$$

We remark that when the modal frequencies are well separated, $\rho_{ij} \approx 0$ and (9) can be simplified as

$$X_{rs} = \sum_{k=1}^{3}\sum_{i=1}^{n} X_{rki}X_{ski}\ , \tag{10}$$

which is the SRSS modal combination rule.

Using the above definitions, the coordinates of the response-spectrum-based envelope bounding two responses in a linear structure are specified as follows. Consider Figure 1, which shows the envelope and a direction vector $\boldsymbol{\alpha} = [\cos\psi, \sin\psi]^T$, where ψ is the counterclockwise angle that $\boldsymbol{\alpha}$ makes with the x_1 axis. Also shown in this figure is the line P_α that has $\boldsymbol{\alpha}$ as its normal vector and is tangent to the envelope. As suggested by the geometry of Figure 1, the tangent point on the envelope in direction $\boldsymbol{\alpha}$ is the point that maximizes the distance, $S_\alpha = \boldsymbol{\alpha}^T\mathbf{x} = x_1\cos\psi + x_2\sin\psi$, of P_α from the origin. As shown by Menun [4], the coordinates of this tangent point are

$$\mathbf{x} = \mathbf{x}_O + \frac{\mathbf{X}\boldsymbol{\alpha}}{\sqrt{\boldsymbol{\alpha}^T\mathbf{X}\boldsymbol{\alpha}}} \tag{11}$$

where $\mathbf{X}$ is a symmetric, positive semi-definite 2×2 “response matrix” whose (r,s) element is X_{rs} defined by (9), or (10) when the modal frequencies are well separated.

For the two-dimensional envelopes considered in this paper, it is convenient to expand (11) as

$$\begin{Bmatrix} x_1 \\ x_2 \end{Bmatrix} = \begin{Bmatrix} x_{O1} \\ x_{O2} \end{Bmatrix} + \frac{1}{X_\alpha}\begin{Bmatrix} X_{11}\cos\psi + X_{12}\sin\psi \\ X_{12}\cos\psi + X_{22}\sin\psi \end{Bmatrix}, \tag{12}$$

where

$$X_\alpha = \sqrt{X_{11}\cos^2\psi + 2X_{12}\sin\psi\cos\psi + X_{22}\sin^2\psi} \tag{13}$$

and we have used the fact that $X_{12} = X_{21}$. The envelope can be generated by evaluating (12) for $0 \le \psi \le 2\pi$ and plotting the resulting $[x_1, x_2]^T$ coordinate pairs. It can be shown (Menun [4]) that, because the response matrix is symmetric and positive semi-definite, the envelope defined by (12) is an ellipse that is centered on $\mathbf{x}_O$.

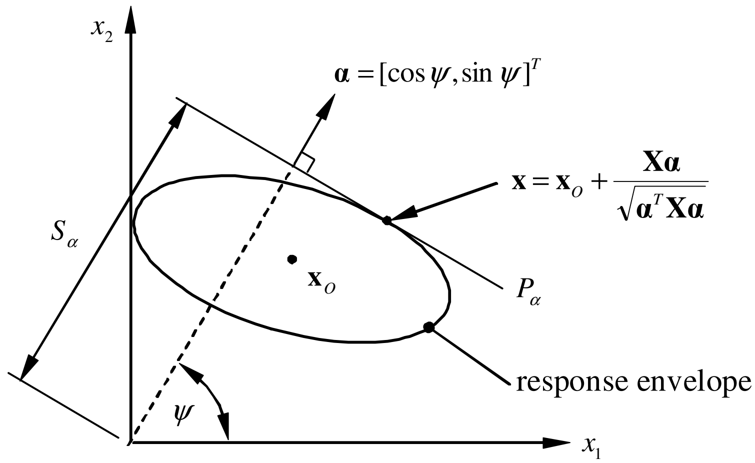

Figure 1. Specification of the coordinates of a response-spectrum-based envelope.

Modification of the response-spectrum-based envelope for nonlinear structures

The response-spectrum-based envelope described in the previous section is only applicable to linear-elastic structures. To predict response envelopes in inelastic structures, the procedure must be modified to account for the effects of any nonlinear behavior. In this paper, we make these modifications by adopting the approach assumed in the MPA procedure [2].

The MPA estimate of the peak value of a seismic response quantity is found by combining the contributions from multiple modes of vibration using the SRSS rule (10) with $r = s$; however, instead of computing the peak modal responses using (8), which assumes the structure remains linear, the MPA procedure computes X_{rki} in a way that incorporates the nonlinear behavior of the structure. That is, the (square of the) MPA estimate of the peak value of $x_{Qr}(t)$ is

$$X_r^2 = X_{rr} = \sum_{k=1}^{3}\sum_{i=1}^{n} X_{rki}^2, \tag{14}$$

in which the peak modal responses X_{rki} are computed as follows.

1. For each component of ground motion, k = 1,2,3, and significant mode of vibration, i = 1,2,…, n, a modal pushover analysis is performed using the load pattern $\lambda\mathbf{s}_{ki}$, where $\lambda \ge 0$ is a scalar constant that is increased until the target displacement, $\delta_{ki} = \delta_{ki}^*$, of a prescribed control node (typically a roof displacement) is attained. During the pushover analysis, the base shear, V_{ki}, and any response quantity of interest, x_r, are recorded as a function of δ_{ki}. We refer to the plots of x_r as a function of δ_{ki} as the pushover database for the analyses.

2. For each modal pushover, the load-displacement curve, V_{ki} - δ_{ki}, is idealized as a bilinear system and normalized by scaling the load axis (V_{ki}) by $[\gamma_{ki}^2(\boldsymbol{\varphi}_i^T\mathbf{M}\boldsymbol{\varphi}_i)]^{-1}$ and the displacement axis (δ_{ki}) by $[\gamma_{ki}\varphi_{ki}]^{-1}$, where φ_{ki} is the element of $\boldsymbol{\varphi}_i$ that corresponds to the control node degree of freedom assumed for ground motion component k. The resulting normalized load-displacement curve

represents the behavior of the inelastic single-degree-of-freedom (SDOF) system associated with the ith mode response of the structure to the kth ground motion component.

3. For the ith mode inelastic SDOF system associated with the kth component of ground motion, the peak displacement, $D_{ki} = \max|d_{ki}(t)|$, is estimated. In practice, this may be done using a design constant-ductility response spectrum.

4. The peak displacement of the control node is computed as $\Delta_{ki} = \gamma_{ki}\varphi_{ki}D_{ki}$. The peak nonlinear modal response, X_{rki}, is that value of x_r that corresponds to $\delta_{ki} = \Delta_{ki}$ in the pushover database assembled in step 1.

To generate the envelope for a pair of responses in a nonlinear structure, we propose that the elements of the response matrix (X_{11}, X_{22} and X_{12}) needed for (12) and (13) be computed using (10) with X_{1ki} and X_{2ki} computed in step 4 of the above procedure rather than with (8). In this way, the nonlinear behavior of the structure is incorporated into the predicted envelope in a manner similar to that used by the MPA procedure for predicting peak scalar response quantities. We remark that the response matrix constructed using (10) with X_{1ki} and X_{2ki} computed in step 4 of the above procedure will be symmetric and positive semi-definite, like the response matrix computed for the linear case; consequently, the proposed envelope for responses in a nonlinear structure will also be an ellipse.

ACCURACY OF THE PROPOSED ENVELOPE

In this section, we examine the accuracy of the proposed envelope for selected pairs of seismic response quantities in a nonlinear structure. In particular, we use the procedures described in the previous section to compute the envelopes that bound (1) the bi-directional inter-story drifts and (2) the axial forces and bending moments in selected columns of a three-story steel-moment-resisting-frame building. These predicted envelopes are then compared to simulated envelopes generated by a set of nonlinear time-history analyses. As a point of comparison, we also plot and compare the predicted and simulated envelopes for the case when the structure remains linear-elastic under the seismic loading. The results obtained for the linear structure provide an indication of how the accuracy of the proposed envelopes for nonlinear structures compares to that achievable for linear structures with the response-spectrum-method. Moreover, the response-spectrum-based linear results give an indication of the level of accuracy that is currently accepted by the profession.

Modeling Considerations

Structure Model

The three-story steel-moment-resisting-frame building shown in Figure 2, which was designed in accordance to the Los Angeles building code and the provisions of FEMA 267 [6] for the second phase of the SAC Joint Venture Steel Project, was used as the focus of this investigation. The geometry, dimensions, material properties and mass of the structure are summarized in Figure 2. The building stiffness and mass are symmetric about both principal axes. Structural nonlinearities in the three-dimensional mathematical model of the building were represented using zero-length plastic hinge elements at the ends of all columns and beams in the perimeter moment frames shown in Figure 2. The moment-rotation relationship for each plastic hinge was represented by a bilinear curve with an initial slope of $k = 20EI/L$, where L is the length of the supported member, and a 0.9 % strain hardening ratio. P-Δ effects are not included in the analyses.

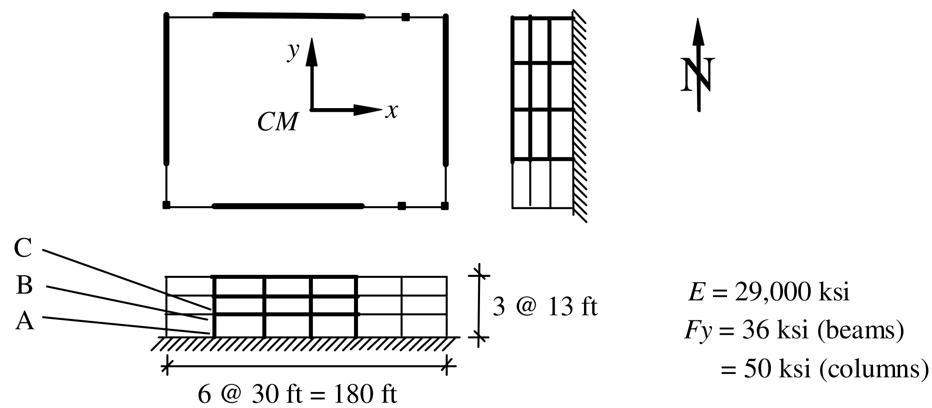

Level	Exterior column	Interior column	Girder	Seismic weight (kips)	Gravity load (psf)
3	W14X257	W14X311	W30X116	1944	90
2	W14X257	W14X311	W30X116	1728	80
1	W14X257	W14X311	W24X62	1728	80

Figure 2. 3-story steel moment-resisting frame building.

Ground Motion Ensemble

An ensemble of 25 pairs of statistically independent artificial ground motions was used to generate the time histories and response spectra needed for the study. These ground motions were applied along the horizontal x- and y-axes of the structure shown in Figure 2. Vertical ground motions were not included in the analyses. The stronger component of each ground motion pair was directed along the x-axis of the structure. In accordance with the observations made by Penzien and Watabe [7], the mean response spectrum of the weaker component of ground was approximately 85% of the mean response spectrum of the stronger component at all frequencies.

The ground motions were simulated as described by Menun [8] such that the mean response spectrum of the ensemble matches a target response spectrum obtained from the Abrahamson and Silva [9] attenuation relationship for rock sites and strike-slip events. The records have intensities and durations that are representative of a M_w = 7.5 earthquake whose rupture plane comes within 2 km of the building site. The statistical properties of the ensemble satisfy the assumptions employed in the development of the response spectrum method; namely, the ground motions are samples of a wide-band, zero-mean Gaussian process that has a stationary strong motion phase that is several times longer than the fundamental period of the building.

Computing and plotting the predicted and simulated envelopes

The mean predicted envelopes plotted below are computed using (12) and (13). For the nonlinear cases, the mean constant ductility response spectra obtained for the strong and weak components of the ground motions are interpolated to determine D_{ki} in step 3 of the MPA procedure described in the previous section. Naturally, for the linear-elastic cases considered, the values of D_{ki} needed to evaluate (8) are obtained directly from the mean displacement response spectra of the ground motion components.

The mean simulated envelopes plotted below are generated as described by Menun [3].

Bi-directional inter-story drifts

The bi-directional inter-story drifts $\Delta_x(t)$ and $\Delta_y(t)$ in the *x*- and *y*-directions, respectively, of the example structure represent the relative displacement between the center nodes of consecutive floors in the building. Plots of the predicted and simulated mean envelopes bounding the bi-directional inter-story drifts at each story of the building are shown in Figure 3 for the linear and nonlinear cases. The predicted linear envelopes shown use the first 5 modes of vibration, and predicted nonlinear envelopes are computed based on the first 2 modes in the x- and y-directions.

From Figure 3, it is apparent that, in contrast to what might be predicted by the equal-displacements rule, significant reductions in the overall sizes of the simulated envelopes occur when the system is allowed to undergo nonlinear behavior. This reduction is thought to be the result of a trade-off between increased effective period and increased effective damping ratio of the structure as it yields. It is noteworthy that the proposed method appears to partially capture this reduction in the size of the nonlinear envelope; however, in all cases, the predicted mean envelope is larger than the simulated mean with a maximum difference of approximately 35% in the Δ_x direction at each story for the nonlinear structure. Compare this level of accuracy to that obtained for the linear structure, in which the maximum difference between the predicted and simulated mean envelopes in any direction is approximately 15%. We also note from Figure 3 that the fact that the proposed method yields an elliptical response envelope is not detrimental to the overall quality of the prediction in this case since the simulated envelopes for the nonlinear system are approximately elliptical.

To further assess the accuracy of the proposed envelope, it is interesting to plot the inter-story drift trajectory $[\Delta_x(t), \Delta_y(t)]^T$ obtained for each nonlinear time-history analysis and the envelope predicted using the actual constant ductility response spectra of the ground motions used. This is done for each of the 25 time-history analyses in Figures 4, 5 and 6. Examining these figures, it appears that, on average, the proposed envelope over-predicts the inter-story drifts as suggested by Figure 3; however, in almost all cases, the trajectory comes very close to the predicted envelope, and sometimes exceeds it, in some directions suggesting that the proposed envelope may in fact be an appropriate upper bound.

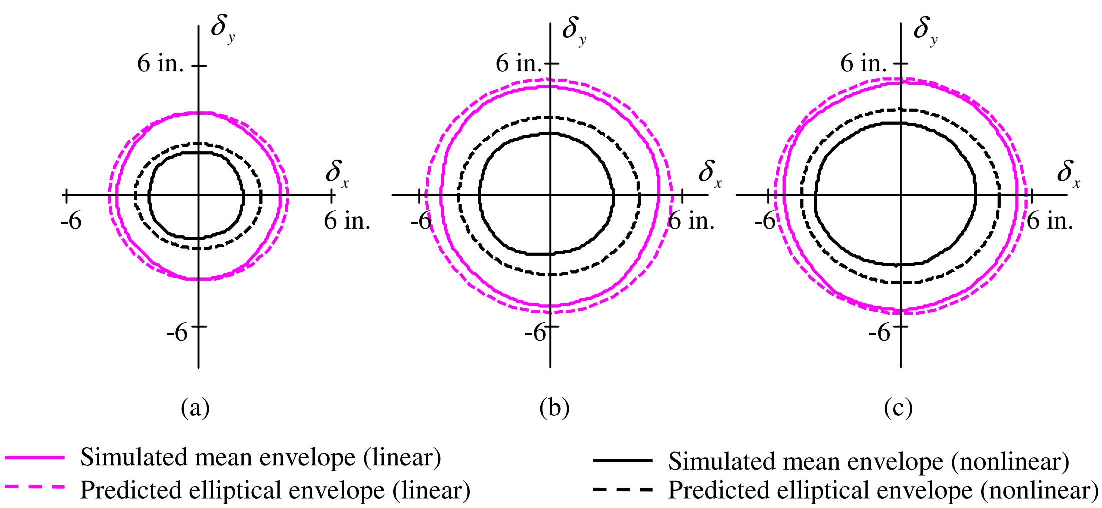

Figure 3. Interstory drift envelope comparisons, simulated vs. predicted, stories 1, 2 & 3.

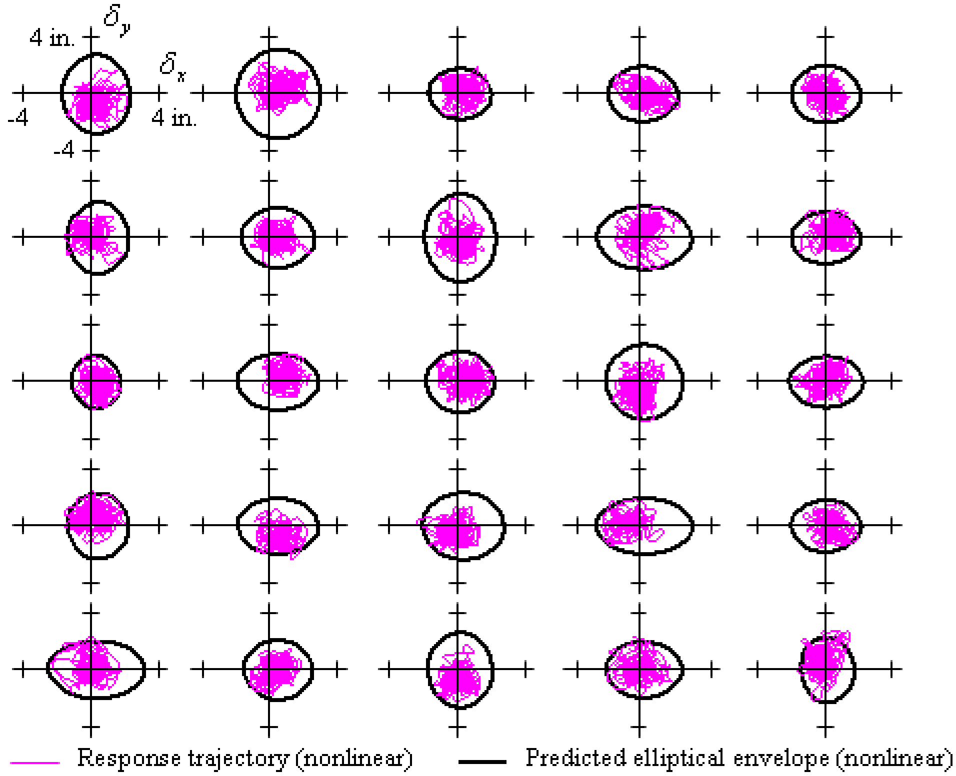

Figure 4. Response trajectories, interstory drifts, story 1.

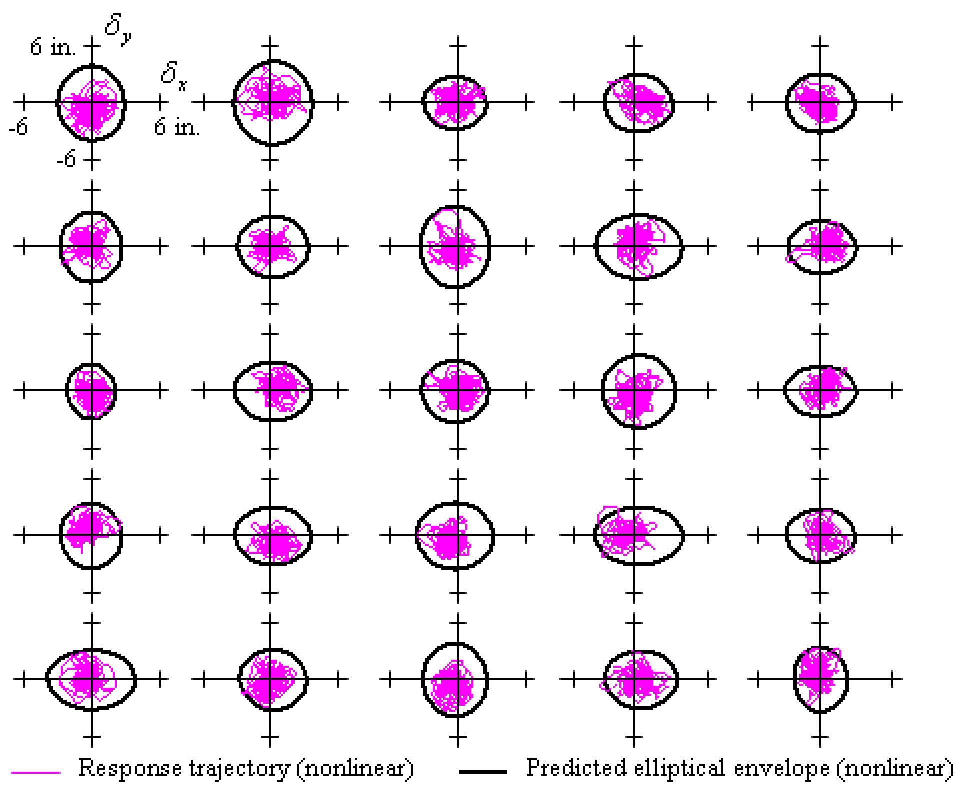

Figure 5. Response trajectories, interstory drifts, story 2.

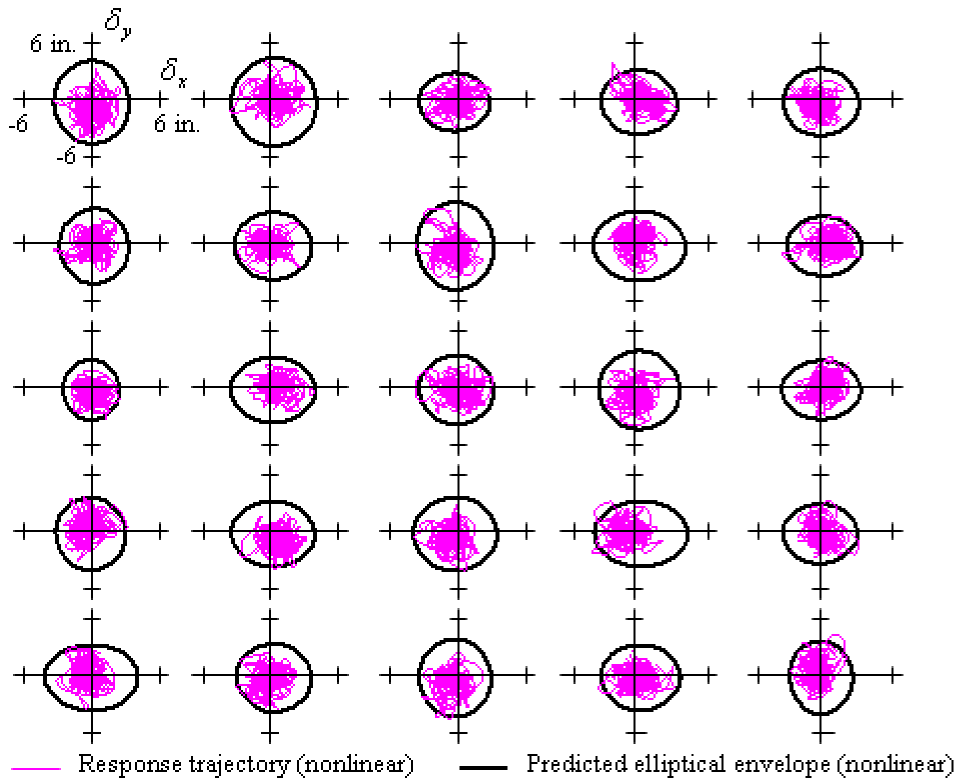

Figure 6. Response trajectories, interstory drifts, story 3.

Axial forces and bending moments in columns

Plotted in Figure 7 are the mean predicted and simulated axial-force-bending-moment (*P-M*) envelopes for the linear and nonlinear cases at the three locations along an exterior column of the E-W moment frame of the example building, which are denoted A, B and C in Figure 2. Predicted linear envelopes were computed using contributions from the first 10 modes of vibration. The first 3 modes in each building direction were used to generate the nonlinear predicted envelopes.

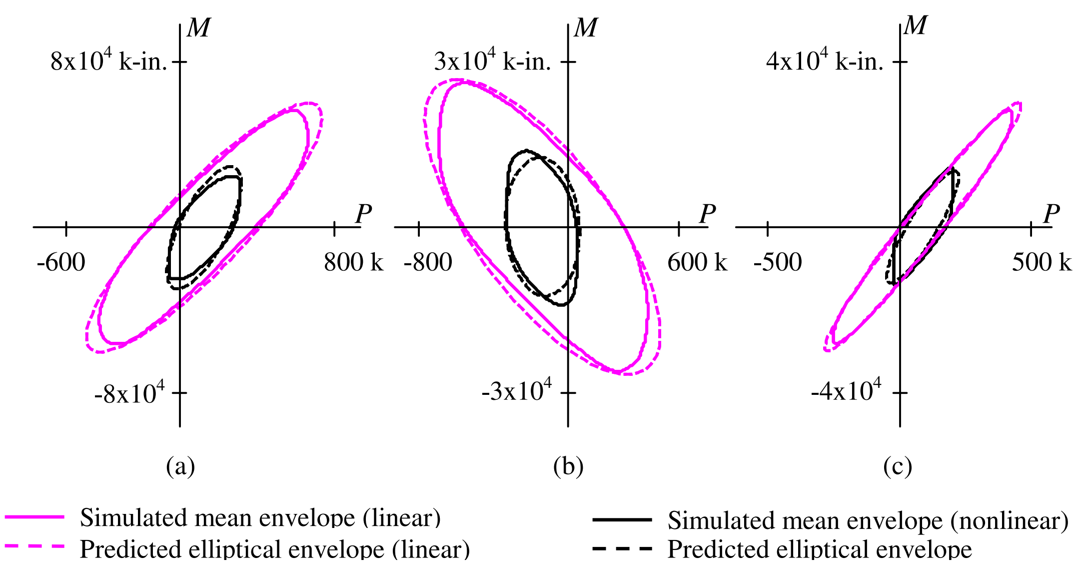

Figure 7. Axial load-bending moment comparisons, simulated vs. predicted, locations A, B & C.

It is apparent in Figure 7 that significant reductions in the overall sizes of the simulated *P-M* envelopes occur when the system experiences nonlinear behavior, which is captured by the predicted envelopes. In fact, the predicted extreme values of the axial forces and bending moments in the nonlinear structure appear to be as accurate as those predicted for the linear structure. However, in contrast to the inter-story drift envelopes, the simulated *P-M* envelope is not elliptical for the nonlinear structure. Straight vertical faces perpendicular to the *P*-axis that act as upper and lower bounds on the axial force can be seen in the simulated envelopes at all locations. Similarly, straight horizontal faces perpendicular to the *M*-axis can also be seen in the simulated envelopes. These flat faces perpendicular to the *P*- and *M*-axes are a result of the plastic hinge capacities at the ends of the beams in the analytical model, which not only limit the maximum bending moment in the beam (and supporting column), but also limits the shear force that acts at the end of the beam, and thus the axial load that can be transmitted to the supporting column. From these *P-M* envelope results, it is evident that the proposed procedure, which always predicts an elliptical envelope, must be modified if we wish to sufficiently capture the distortion seen in the simulated *P-M* envelopes for the nonlinear structure.

Again, to help assess the accuracy of the proposed procedure, it is useful to plot the *P-M* trajectories for each nonlinear time-history analysis and the envelope predicted using the actual constant ductility response spectra of the ground motions used. These trajectory plots and envelopes are shown in Figures 8, 9 and 10. The results presented in these figures suggest that, on average, the proposed envelope provides a reasonable bound on the *P-M* trajectory that is appropriate for seismic design and analysis.

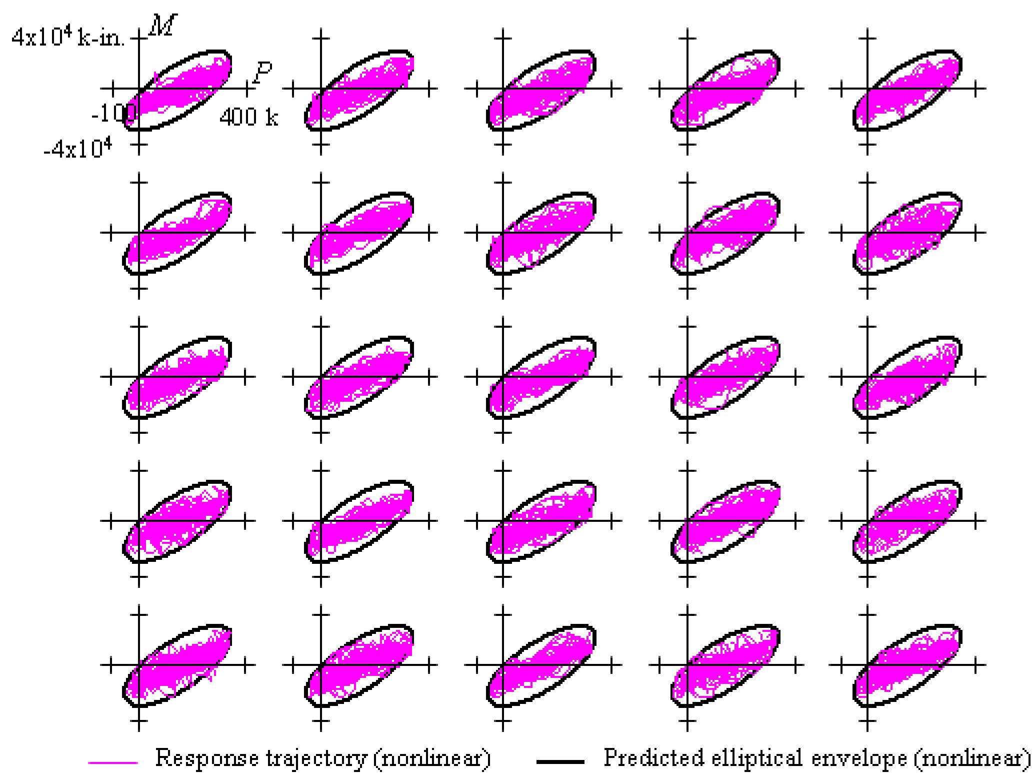

Figure 8. Response trajectories, axial load-bending moment, location A.

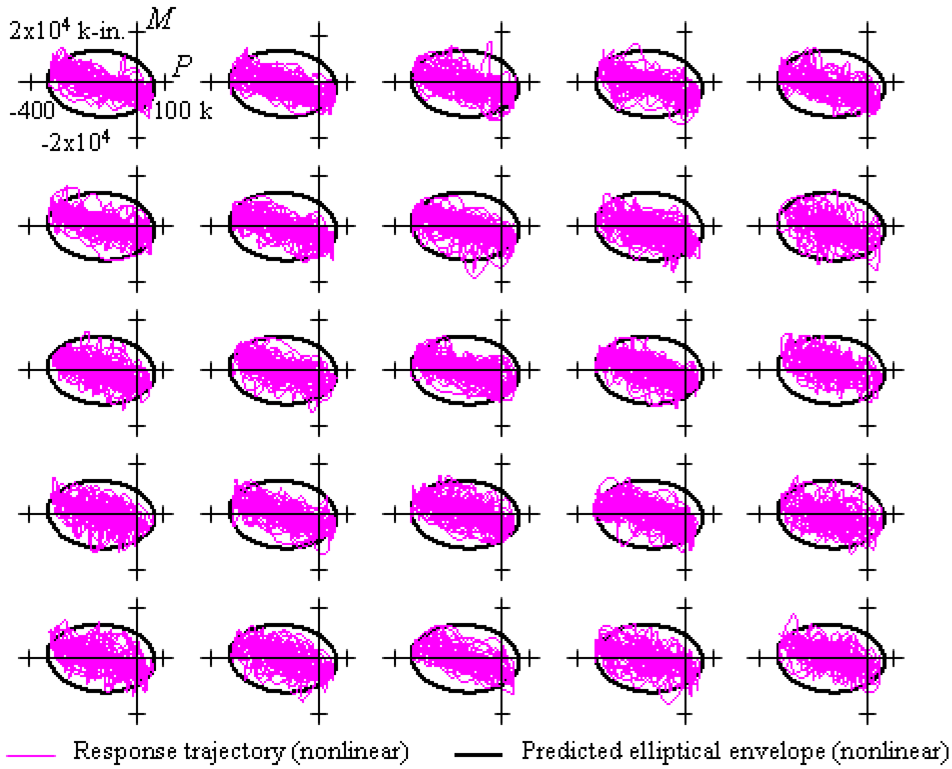

Figure 9. Response trajectories, axial load-bending moment, location B.

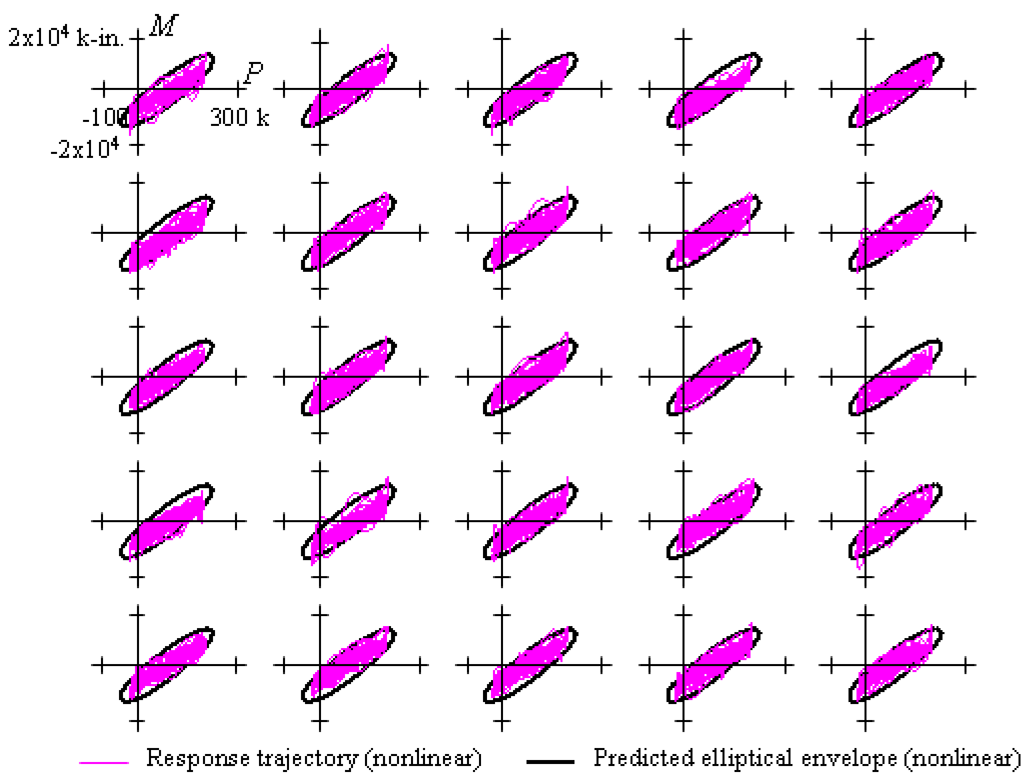

Figure 10. Response trajectories, axial load-bending moment, location C.

CONCLUSIONS

A method has been presented for predicting the envelope that bounds a pair of seismic responses in a nonlinear structure. The proposed procedure is based on the response-spectrum-based envelope developed by Menun [4] for linear structures with modifications to account for the effects of material nonlinearities. In particular, the conventional response-spectrum-based estimates for the peak modal responses used in the formulation of the envelope for linear structures are replaced with the peak modal responses predicted by the MPA procedure developed by Chopra [2].

The accuracy of the proposed envelope was examined for (1) the bi-directional inter-story drifts and (2) the axial forces and bending moments in selected columns of a three-story steel-moment-resisting-frame building. To assess the accuracy of the proposed method, the predicted envelopes using the proposed method were compared to simulated envelopes generated from nonlinear time-history analyses. Simulated and predicted response envelopes for linear structures were also plotted to provide an indication of how the accuracy of the proposed envelopes for nonlinear structures compares to that achievable for linear structures with the response-spectrum-method.

The inter-story drift envelope comparisons showed that maximum drifts in the nonlinear system were overestimated by the procedure by as much as 35% on average; however, the elliptical shape of the predicted envelopes was comparable to that seen in the simulated envelopes. The opposite was found for the axial-force-bending-moment envelopes: the predicted values of axial force and bending moment were close to the maximum simulated values, but the shape of the simulated envelope did not resemble an ellipse, which is the shape predicted by the proposed procedure. The distortion seen in the simulated axial-force-bending-moment envelopes for the nonlinear system was due to the maximum possible values of bending moment and axial load that could be transmitted to the column through the plastic hinges at the ends of the girders in the nonlinear system. Modifications to the proposed procedure to account for the non-elliptical shape of the axial-force-bending-moment envelopes are currently being examined.

REFERENCES

1. FEMA 273. “NEHRP guidelines for the seismic rehabilitation of buildings.” Washington DC: Federal Emergency Management Agency, 1997.
2. Chopra AK, Goel RK. “A modal pushover analysis procedure to estimate seismic demands for buildings.” PEER Report 2001/03. Berkeley: Pacific Earthquake Engineering Center, University of California Berkeley, 2001.
3. Menun C, Der Kiureghian A. “Envelopes for seismic response vectors. II: Application.” Journal of Structural Engineering 2000; 126: 474-481.
4. Menun C, Der Kiureghian A. “Envelopes for seismic response vectors. I: Theory.” Journal of Structural Engineering 2000; 126: 467-473.
5. Chopra AK. “Dynamics of Structures: Theory and Applications to Earthquake Engineering, 2nd edition.” New Jersey: Prentice Hall, 2001.
6. FEMA 267. “Interim guidelines: evaluation, repair, modification and design of welded steel moment frame structures.” Washington DC: Federal Emergency Management Agency, 1995.
7. Penzien J, Watabe M. “Characteristics of three-dimensional earthquake ground motion.” Earthquake Engineering and Structural Dynamics 1975; 3: 365-374.
8. Menun C, Der Kiureghian A. “Envelopes for Seismic Response Vectors.” *PEER Report 1999/08*. Berkeley: Pacific Earthquake Engineering Center, University of California Berkeley, 1999.
9. Abrahamson N and Silva WJ. “Empirical response spectral attenuation relations for shallow crustal earthquakes.” Seismological Research Letters 1997; 68: 94-127.